ChemComm

COMMUNICATION

View Article Online
View Journal | View Issue

Cite this: *Chem. Commun.*, 2020, **56**, 5382

Received 28th October 2019,
Accepted 6th April 2020

DOI: 10.1039/c9cc08419c

rsc.li/chemcomm

Molecular nanoparticles of cerium dioxide: structure-directing effect of halide ions†

Bradley Russell-Webster, Khalil A. Abboud and George Christou *

The use of halide ions in the synthesis of Ce/O clusters diverts the reaction to two halide-containing products: Cl^- gives a new Ce_{20} nuclearity with both a high 1 : 1 Ce^{3+} : Ce^{4+} ratio and a high percentage of (100) facet coverage, whereas F^- gives a known Ce_6 nuclearity. Both products include bridging halide ions and are thus the first confirmation of non-oxo (OH^-/O^{2-}) anion incorporation onto the Ce/O cluster core.

Cerium dioxide (CeO_2, ceria) has been widely used since the 1970's in three-way catalytic converters, functioning as both a support and an oxygen buffer.[1–5] Since then the uses of ceria have increased dramatically across a wide front, spanning industrial catalysis,[6] solid oxide fuel cells,[7] chemical mechanical polishing,[8] UV filters,[9] and others. These diverse applications reflect versatile reactivity modes arising from the Ce^{3+}/Ce^{4+} redox couple and ceria's ability to both absorb and release O depending on its chemical environment, allowing it to exist in a range of oxides from fully oxidized CeO_2 to fully reduced Ce_2O_3.

More recently ceria nanoparticles (CNPs) have been attracting great interest owing to their increased reactivity at lower temperatures than their bulk counterparts.[10] This has also included room temperature, opening up new biomedical applications of ultra-small (<20 nm) CNPs, functioning as enzyme mimics and scavengers of reactive oxygen species (ROS).[11–14] These behaviours can be attributed to the decrease in CNP size leading to an increase in the concentration of surface Ce^{3+} and concomitant 'O-vacancy' defect sites.[15,16] The activity of the CNPs is also found to be facet-dependent, and thus it is highly desirable to develop synthetic control to enhance the CNP content of specific facets.[17–19] CNPs display three thermodynamically stable low-index facets: (111), (110) and (100). The stability of these facets has been assessed using density functional theory (DFT) calculations and was found to decrease in the order (111) > (110) > (100).[18] As a result, the redox catalytic activity follows the opposite trend owing to the ease with which the (110) and (100) facets are able to form O-vacancies.[20–22] Under thermodynamic control the most stable facets are formed, and this often leads to the isolation of CNPs with octahedral and/or truncated octahedral shapes rich in (111) facets. To synthesize CNPs with enhanced content of the more reactive (110) and (100) facets, kinetic control must be imposed,[23] and there are two methods commonly employed for this: (i) capping agents, and (ii) template-assisted synthesis.[4] Capping agents are found to interact with a specific crystallographic plane, altering surface free energies and favoring the growth in a particular direction. This has been seen in the synthesis of CeO_2 nanocubes where NO_3^- ions selectively interact with (100) facets and favour their growth.[24] Templating is able to restrict the growth of the CNPs during the Ostwald ripening by the use of surfactants.[25]

We recently published a family of Ce/O clusters with primarily carboxylate ligation and Ce nuclearities ranging from 24 to 40. These clusters possess the same fluorite structure as bulk cerium dioxide and are thus what we are now calling "molecular nanoparticles", *i.e.*, ultra-small CNPs obtained in molecular form and thus possessing the molecular advantages of true monodispersity (single-size), solubility and crystallinity, allowing structural characterization to atomic precision by single-crystal X-ray crystallography. As expected, their surfaces are primarily composed of thermodynamically stable (111) facets.[26] These molecular nanoparticles have helped shed light on surface structural features of CNPs, such as the locations and environments of Ce^{3+} and H^+ ions, the nature of O-vacancy sites, and the effect of the ligand upon the nuclearity of the Ce/O molecular nanoparticle. We feel these truly monodisperse molecular complexes thus represent a powerful bottom-up route to ultra-small nano-ceria, especially for biomedical applications where <20 nm CNPs are desirable.[27] None of our clusters contained any non-O ions in their Ce/O core. In the present work, we report a new synthetic procedure to Ce/O clusters that includes F^- and Cl^- ions, and we show that these halide ions are incorporated into the core, whilst maintaining the same carboxylate ligand shell, giving a new Ce_{20} cluster with Cl^-

Department of Chemistry, University of Florida, Gainesville, FL 32611-7200, USA. E-mail: christou@chem.ufl.edu

† Electronic supplementary information (ESI) available: Synthetic procedures, crystallographic and other characterization details for complexes **1** and **2**. CCDC 1897929 and 1897930. For ESI and crystallographic data in CIF or other electronic format see DOI: 10.1039/c9cc08419c

with an unusually high content of (100) facets, and with F^- the first Ce/O/F cluster.[26]

We initially investigated addition of organic salts of Cl^- and F^- into the synthetic procedure in aqueous pyridine reported by Mitchell *et al.*,[26] but in this solvent mixture we found no halide incorporation into the products. We thus developed a new procedure in MeCN to the desired materials. The reaction of $CeCl_3$, $PhCO_2H$, pyridine, and $(NH_4)_2[Ce(NO_3)]_6$ in a 0.5 : 1.0 : 4.4 : 0.1 molar ratio in MeCN gave a light purple solution from which were obtained after four weeks purple crystals of $(pyH)_3(NH_4)[Ce_{20}O_{18}Cl_{16}(O_2CPh)_{22}]$ (**1**). No F-containing product could be isolated when $CeCl_3$ was replaced with CeF_3; however, the reaction of CeF_3, $PhCO_2H$, pyridine and $(NH_4)_2[Ce(NO_3)]_6$ in a 0.5 : 1.0 : 4.4 : 0.1 molar ratio in MeCN, heated at 80 °C for one hour in a Biotage Initiator microwave reactor, gave a light-yellow solution from which bright yellow crystals of $[Ce_6O_4(OH)_3F(O_2CPh)_{12}py_2]$ (**2**) were obtained. No Br-containing product could be successfully isolated when $CeBr_3$ was used in place of $CeCl_3$ or CeF_3.

The anion of **1** contains a $[Ce^{III}{}_{10}Ce^{IV}{}_{10}(\mu_4\text{-}O^{2-})_{14}(\mu_3\text{-}O^{2-})_4(\mu_4\text{-}Cl)_8(\mu_2\text{-}Cl)_8]^{18+}$ core (Fig. 1). There is a central $\{Ce^{IV}{}_{10}O_{14}\}$ unit comprising an edge-linked Ce_{10} bioctahedron bridged by O^{2-} ions, at each end of which is attached a $\{Ce^{III}{}_5O_2\}$ unit, the reduced O^{2-} content in the latter favouring the lower Ce^{III} oxidation state. The Ce oxidation states and core O protonation levels were confirmed using bond valence sum (BVS) calculations (Tables S2 and S3, ESI†).[28a] The core has the layered fluorite structure of bulk CeO_2 and is thus a new member of the family of molecular nanoparticles of this material, but with an unusually high content of surface Ce^{III}. The Cl^- ions are all attached in bridging modes to the surface of the $\{Ce_{20}O_{18}\}$ unit, and the ligation is completed by a shell of μ-$PhCO_2^-$ groups that adopt two binding modes: 12 are $\eta^2{:}\eta^1{:}\mu_2$ and the remaining 10 are $\eta^1{:}\eta^1{:}\mu_2$. Three pyridinium cations were crystallographically located hydrogen-bonding to surface Cl^- ions, but the fourth cation was concluded to be within a region of much disordered solvent and was assigned as NH_4^+ (or H_3O^+) on the basis of the elemental analysis data (see ESI†).

Analysis of the surface identifies it to comprise both (111) and (100) facets, with a much larger number (6) of the latter than in previous Ce/O clusters (Fig. 2).[26] In the Ce/O molecular nanoparticles reported by Mitchell *et al.*, the (100) facets are either separated from one another or connected at a single atom atom (typically Ce^{III} ion).[26] Complex **1** contains instead the first example of two pieces (squares) of (100) facets fused through an edge to create a (100) facet with a greater surface area. All (100) facets are bridged by a μ_4-Cl^- ion and they all contain at least two Ce^{III} ions, consistent with previous observations that Ce^{III} favours these facets.[26] In addition, the Ce–Cl bond distances (2.9–3.1 Å) are reasonable for μ_4-Cl bonding to Ce, in contrast to similar distances for μ_4-O bridging by OH^- or carboxylate O atoms that are long and which we therefore previously described as weakly-interacting 'lids' on the (100) facets.[26] Both Cl^- and OH^- ions have been concluded from DFT calculations by Chen *et al.*[28] to be able to stabilize (100) facets in bare nanoparticles. Although these molecular nanoparticles are not organic ligand-free, the DFT results allow us to draw inferences

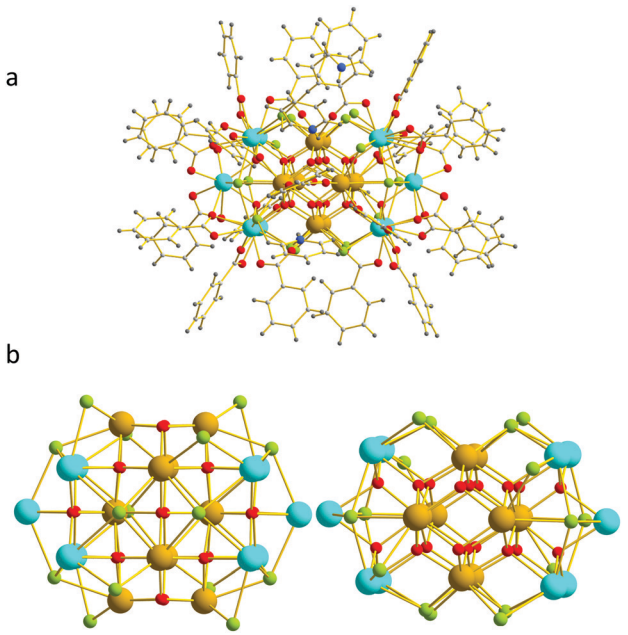

Fig. 1 (a) The complete structure of the anion of **1**, and (b) its $Ce_{20}O_{18}Cl_{16}$ core from two viewpoints differing by rotation about the horizontal axis. Colour code: Ce^{IV} gold, Ce^{III} sky blue, O red, Cl green, N blue, C light grey, H dark grey.

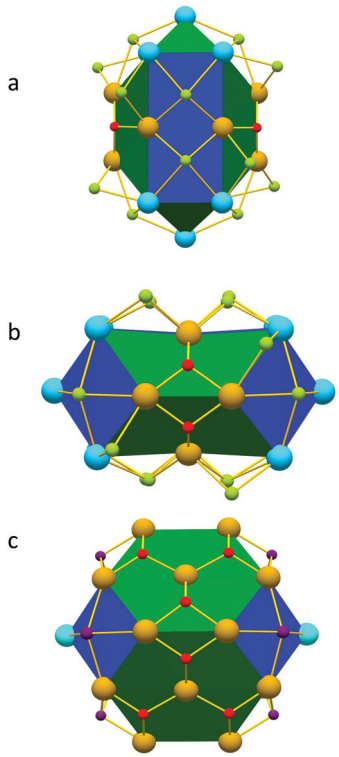

Fig. 2 (a and b) The Ce_{20} anion of **1** from two perpendicular viewpoints, with the benzoate ligands omitted for clarity. Facets are colour coded: (100) blue, (111) green. The μ_4-Cl^- ions bridge (100) facets, whereas μ_2-Cl^- ions bridge edges linking (111) (100) facets. (c) The Ce_{24} cluster from the same viewpoint as in (b), and with benzoate and py ligands omitted, Colour code: Ce^{IV} gold, Ce^{III} sky blue, O red, OH^- purple, Cl green.

about potential anions that may stabilize (100) facets.[28] We have already seen experimentally that OH^- ions can stabilize (100) facets in Ce/O molecular nanoparticles,[26] and it is reasonable that this should also be possible by another anion (*i.e.*, Cl^-) proposed in the DFT study. Indeed, **1** now provides the first crystallographic evidence for Cl-binding preferences and modes to the surface facets of the fluorite lattice. All the remaining 8 Cl^- ions adopt a μ_2-bridging mode on $Ce^{III}Ce^{IV}$ pairs at the intersection of (100) and (111) facets.

Further comparison shows the anion of **1** to be structurally related to the reported $[Ce_{24}O_{28}(OH)_8(PhCO_2)_{30}(py)_4]$ cluster (Fig. 2c), which has an **A**:**B**:**C**:**B**:**A** five-layer structure of Ce atoms and contains only four (100) facets.[26] The anion of **1** (Fig. 2b) can be seen to be the Ce_{24} stucture with the top and bottom **A** layers removed (as well as its attendant layer of O^{2-} and OH^- ions, Fig. S1, ESI†), with μ_2- and μ_4-Cl^- ions binding to the resulting (100) facets. This suggests that the Cl^- ions have inhibited growth of the cluster in this vertical direction by stabilizing the (100) facets in layer **B** and disfavouring additional Ce and O^{2-} attachment to them. Thus coordination of the μ_2-Cl^- ions in **1** appears to block the addition of Ce ions to the **B** layer, inhibiting the growth to the Ce_{24}. The resulting decrease in surface O^{2-} ions also rationalizes the greater Ce^{III} content in these (100) facets and the Ce_{20} as a whole (Ce^{III}:Ce^{IV} = 1:1 and 1:12 in Ce_{20} and Ce_{24}, respectively); the Ce^{III} and Ce^{IV} ions are coordinated to 2 and 4 or more O^{2-} ions, respectively.

The structural similarity between Ce_{20} and Ce_{24} is evident in the root-mean-square (RMS) deviation analysis (Fig. S2 and Table S4, ESI†). As expected, the significant deviations are primarily assignable to Ce positions that are Ce^{3+} and Ce^{4+} in Ce_{20} and Ce_{24}, respectively, and the Cl bridges in Ce_{20}, particularly the μ_2-Cl^- ions present at the (100) (111) facet intersections.

Complex **2** is a Ce_6 cluster with a distorted octahedral topology that is a small but nevertheless recognizable unit within the CeO_2 fluorite structure (Fig. 3); the core surface contains only small (111) facets. Similar Ce_6 clusters have been previously reported from a variety of synthetic procedures; in all cases, each face of the Ce_6 octahedron is μ_3-bridged by an O^{2-} or OH^- ion, but the total O^{2-}/OH^- count has varied, *i.e.*, $O_{8-x}(OH)_x$.[29–32] For **2**, which lies on an inversion centre, the crystallographic study identified the overall structure of the cluster but given the similar charge, size and bond lengths to Ce of F^- *vs.* OH^- ions it cannot by itself confirm the presence of F^-. Instead, the core was concluded to be $[Ce_6O_4(OH)_3F]$ by a combination of the following: (i) the overall charge balance in the neutral cluster; (ii) the elemental analysis of 1 F per Ce_6 cluster; (iii) the refinement of the four bridging core O atoms (of the asymmetric unit) giving isotropic displacement parameters with values too high, and further refinement resolving them into two sets of O atoms assignable to O^{2-} *vs.* OH^- but with occupancies for each set refining to over 0.5 (each 0.54, greater than the expected total of 1.0); (iv) on the basis of the F analysis, the inclusion of one F^- at the OH^- positions leading to an improvement in the refinement with O^{2-}/OH^-/F^- occupancies of 0.54/0.345/0.115 (R_1/wR_2 = 2.99/7.37% *vs.* 3.33/7.92%) corresponding to a $[Ce_6O_4(OH)_3F]$ core; and (v) O BVS calculations that gave values of ~2.0 for one set consistent with O^{2-} ions, and ~1.2 for the other, at the upper end of the range for OH^- (Table S3, ESI†). Unlike the Cl^- ions in the anion of **1**, which adopt both μ_2 and μ_4 bridging modes, the F^- thus adopts a μ_3 mode. The structure of **2** is completed by 12η^1:η^1:μ_2 benzoate groups and 2 pyridine ligands.

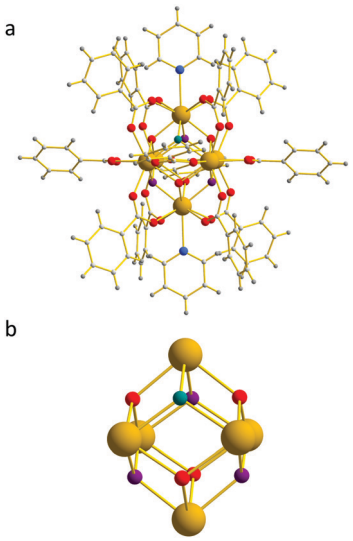

Fig. 3 (a) The complete structure of **2**, and (b) the $[Ce_6O_4(OH)_3F]$ core with only one set of disorder positions shown for clarity. Colour code: Ce^{IV} gold, O red, OH purple, F teal, N blue, C light grey, H dark grey.

In summary, initial investigation of the effect of halide ions on the obtained Ce/O molecular nanoparticles has led to isolation and structural characterization to atomic detail of halides bound to Ce/O fluorite surface features. Product **1** is particularly interesting, demonstrating a structure-directing effect of Cl^- to give a product that can be described as resulting from inhibited growth in one direction by stabilization of (100) facets. Since the latter are known to be highly active sites in catalysis by nanoscale CeO_2,[33] their resulting high concentration in **1** due to Cl^- suggests a means of obtaining molecular nanoparticles that may display enhanced catalytic activities as-is and/or once the carboxylate ligand shell is removed under mild conditions. Note that removal of the organic shell is often not a prerequisite for catalytic activity, either in CNPs or molecular clusters. Indeed, for biomedical applications in aqueous media such as catalytic radical scavenging, CNPs with organic shells of, *e.g.*, polyethylene glycol[34] or dextran[35] provide water solubility and protection from aggregation/agglomeration while still yielding excellent radical scavenging activities. Similarly, we have found high catalytic radical scavenging by our Ce_x molecular clusters with carboxylate ligation.[36]

Further studies are in progress to extend the work to Br^- and other small anions, as well as broadening the present work. For example, the μ_3-F^- in **2** is analogous to the common surface μ_3-O^{2-} and –OH^- ions in Ce/O molecular nanoparticles. Since DFT calculations have concluded that F^- and OH^- have a similar stabilization energy on a (100) facet of bare Ce/O nanoparticles,[28] we thus hope to encounter a μ_4-F on a (100) in future work.

We thank the U.S. National Science Foundation for funding (CHE-1900321). KAA acknowledges the National Science

Foundation and the University of Florida for funding the purchase of the X-ray equipment.

Conflicts of interest

There are no conflicts to declare.

Notes and references

1 M. Flytzani-Stephanopoulos, *MRS Bull.*, 2001, **26**(11), 885–889.
2 Q. Wang, B. Zhao, G. Li and R. Zhou, *Environ. Sci. Technol.*, 2010, **44**, 3870–3875.
3 A. Trovarelli, *Catal. Rev.*, 1996, **38**, 439–520.
4 T. Montini, M. Melchionna, M. Monai and P. Fornasiero, *Chem. Rev.*, 2016, **116**(10), 5987–6041.
5 H. C. Yao and Y. F. Y. Yao, *J. Catal.*, 1984, **86**(2), 254–265.
6 A. Trovarelli, C. de Leitenburg, M. Boaro and G. Dolcetti, *Catal. Today*, 1999, **50**(2), 353–367.
7 L. Fan, C. Wang, M. Chen and B. Zhu, *J. Power Sources*, 2013, **234**, 154–174.
8 L. M. Cook, *J. Non-Cryst. Solids*, 1990, **120**, 152–171.
9 K. Reed, A. Cormack, A. Kulkarni, M. Mayton, D. Sayle, F. Klaessig and B. Stadler, *Environ Sci.: Nano*, 2014, **1**, 390–405.
10 T. Tabakova, F. Boccuzzi, M. Manzoli, J. W. Sobczak, V. Idakiev and D. Andreeva, *Appl. Catal., A*, 2006, **298**, 127–143.
11 C. Korsvik, S. Patil, S. Seal and W. T. Self, *Chem. Commun.*, 2007, 1056–1058.
12 Y. Xue, Q. Luan, D. Yang, X. Yao and K. Zhou, *J. Phys. Chem. C*, 2011, **115**(11), 4433–4438.
13 T. Pirmohamed, J. M. Dowding, S. Singh, B. Wasserman, E. Heckert, A. S. Karakoti, J. E. S. King, S. Seal and W. T. Self, *Chem. Commun.*, 2010, **46**, 2736–2738.
14 S. Babu, A. Velez, K. Wozniak, J. Szydlowska and S. Seal, *Chem. Phys. Lett.*, 2007, **442**, 405–408.
15 S. Tsunekawa, T. Fukuda and A. Kasuya, *J. Appl. Phys.*, 2000, **87**, 1318–1321.
16 S. Tsunekawa, R. Sivamohan, S. Ito, A. Kasuya and T. Fukuda, *Nanostruct. Mater.*, 1999, **11**, 141–147.
17 E. Aneggi, D. Wiater, C. de Leitenburg, J. Llorca and A. Trovarelli, *ACS Catal.*, 2014, **4**(1), 172–181.
18 A. Trovarelli and J. Llorca, *ACS Catal.*, 2017, **7**(7), 4716–4735.
19 D. Zhang, X. Du, L. Shi and R. Gao, *Dalton Trans.*, 2012, **41**, 14455–14475.
20 J. C. Conesa, *Surf. Sci.*, 1995, **339**, 337–352.
21 T. X. T. Sayle, S. C. Parker and C. R. A. Catlow, *Surf. Sci.*, 1994, **316**, 329–336.
22 T. X. T. Sayle, M. Molinari, S. Das, U. M. Bhatta, G. Möbus, S. C. Parker, S. Seal and D. C. Sayle, *Nanoscale*, 2013, **5**, 6063–6073.
23 C. Burda, X. Chen, R. Narayanan and M. A. El-Sayed, *Chem. Rev.*, 2005, **105**(4), 1025–1102.
24 Q. Wu, F. Zhang, P. Xiao, H. Tao, X. Wang, Z. Hu and Y. Lü, *J. Phys. Chem. C*, 2008, **112**(44), 17076–17080.
25 K.-S. Lin and S. Chowdhury, *Int. J. Mol. Sci.*, 2010, **11**(9), 3226–3251.
26 K. J. Mitchell, K. A. Abboud and G. Christou, *Nat. Commun.*, 2017, **8**, 1445.
27 S. Das, J. M. Dowding, K. E. Klump, J. F. McGinnis, W. Self and S. Seal, *Nanomedicine*, 2013, **8**, 1483–1508.
28 (*a*) I. D. Brown, *Chem. Rev.*, 2009, **109**(12), 6858–6919; (*b*) Y. Chen, S. Lv, C. Chen, C. Qiu, X. Fan and Z. Wang, *J. Phys. Chem. C*, 2014, **118**(8), 4437–4443.
29 R. Das, R. Sarma and J. B. Baruah, *Inorg. Chem. Commun.*, 2010, **13**(6), 793–795.
30 S. L. Estes, M. R. Antonio and L. Soderholm, *J. Phys. Chem. C*, 2016, **120**(10), 5810–5818.
31 L. Mathey, M. Paul, C. Copéret, H. Tsurugi and K. Mashima, *Chem. – Eur. J.*, 2015, **21**(38), 13454–13461.
32 C. Hennig, A. Ikeda-Ohno, W. Kraus, S. Weiss, P. Pattison, H. Emerich, P. M. Abdala and A. C. Scheinost, *Inorg. Chem.*, 2013, **52**(20), 11734–11743.
33 K. Zhou, X. Wang, X. Sun, Q. Peng and Y. Li, *J. Catal.*, 2005, **229**(1), 206–212.
34 A. S. Karakoti, S. Singh, A. Kumar, M. Malinska, S. V. N. T. Kuchibhatla, K. Wozniak, W. T. Self and S. Seel, *J. Am. Chem. Soc.*, 2009, **131**, 14144–14145.
35 J. M. Perez, A. Asati, S. Nath and C. Kaittanis, *Small*, 2008, **4**, 552–556.
36 K. J. Mitchell, J. Goodsell, U. Twahir, A. Angerhofer, K. A. Abboud and G. Christou, manuscript in preparation.